International Journal of ChemTech Research
CODEN(USA): IJCRGG ISSN : 0974-4290
Vol.4, No.4, pp 1282-1294, Oct-Dec 2012

The Effect of 100 MeV Oxygen Ions on Electrical, Mechanical and Optical Properties of Nonlinear Optical L-Alanine Sodium Nitrate (LASN) Single Crystals

M A Ahlam and A P Gnana Prakash*

Department of Studies in Physics, University of Mysore, Manasagangotri, Mysore-570006, Karnataka, India

Corres. Author: gnanaprakash@physics.uni-mysore.ac.in / omaymn771@gmail.com
Ph.No.+91-9590583920/9449223826

Abstract: Single crystals of nonlinear optical (NLO) L-alanine sodium nitrate (LASN) were grown by slow evaporation method at room temperature. For the first time, the grown crystals were irradiated by 100 MeV oxygen ions with the cumulative doses of 1 Mrad, 6 Mrad and 10 Mrad. The powder X-ray diffraction analysis, optical and dielectric properties, AC and DC conductivity, differential scanning calorimetry (DSC), refractive index (RI), mechanical properties and second harmonic generation (SHG) of the crystals were studied before and after irradiation. The intensity of peaks in diffraction patterns was observed to change in irradiated crystals and there is no significant formation of intermediate chemically distinct material after irradiation. The irradiation induced defect at the crystal surface becomes more prominent at higher irradiation doses, leading to the enhancement in the optical absorption behaviour. The dielectric constant, AC and DC conductivity of the crystals were found to increase after irradiation. The DSC studies reveal that the melting point remains unaffected due to irradiation and the crystals does not decompose as a result of irradiation. A considerable change in the values of RI was observed after irradiation. The SHG efficiency of LASN was found to decrease with increase in ion dose.
Keywords: Ion irradiation, nonlinear optical, irradiation effect, DSC, SHG.

1. INTRODUCTION

NLO materials play a major role in nonlinear optics and getting attention in the field of optical data storage, telecommunication, second harmonic generation (SHG) and optical signal processing. After the advent of laser, the nonlinear phenomena made a big revolution in the field of optics and the frequency conversion become an important and popular for laboratory lasers (1-3). Many of the solid-state lasers are designed to work in the strong external fields of ionizing radiation for space born applications; therefore it is essential to know whether the used components in these lasers sustain the exposure to space radiation which can cause damage as ionization of atoms and structural damage of the laser material (4-6). Therefore study the effects of different radiations on solid state materials in particular NLO crystals is the only way of understanding degradation mechanisms, estimation of the lifetime of the crystals in different environments and possible reducing a radiation damage of

devices. It was shown that swift heavy ion irradiation on crystalline materials are changing its physical and chemical properties of the specimens (7-13). When high energy swift heavy ion passes through matter; it loses its energy mainly in two ways. The interaction of heavily charged ions with electrons of the target material produces a track of ionization and highly kinetic electrons along the path of the primary ion due to inelastic collision. This is known as electronic energy loss or electronic stopping. Nuclear energy loss or nuclear stopping caused by the elastic scattering from the nuclei of the atoms. It is dominant near the end of the range of implanted ions and spent in displacing atoms of the sample. The energy deposited in electronic excitation may result in the creation of defects and modification the material properties (7-9, 14-18). Depending on ion kinetic energy, mass and nuclear charge, an ion can create changes within a thin surface layer or can penetrate far into the bulk to produce long and narrow zone along its trajectory (18, 19). The swift heavy ion irradiation recently has been widely used as a powerful technique to change the refractive index of the crystals, by which waveguides can be therefore fabricated (20- 22). In this paper we made an attempt to understand the effect of swift heavy ion irradiation on LASN nonlinear optical single crystal. LASN is semiorganic nonlinear optical single crystal possess several attractive properties such as high laser damage threshold, wide transparency range, high mechanical strength and thermal stability makes it suitable for second harmonic generation (SHG), laser spectroscopy, laser processing and other NLO applications. LASN crystal possess an orthorhombic system with noncentrosymmetric space group $P2_12_12$ with lattice parameters a = 6.127 Å, b = 12.394 Å, C = 5.797 Å (23, 24). For the first time, we present the results of 100 MeV O^{7+} ions irradiation effects on electrical, mechanical and optical properties of LASN crystal.

2. EXPERIMENTAL DETAILS

The single crystals of LASN were synthesized from L-alanine and sodium nitrate taken in the equi-molar ratio. The calculated amounts of the reactants were dissolved in double distilled water and stirred well for about 3 hours using a magnetic stirrer at 50°C to form a saturated solution. The solution was then filtered twice to remove the suspended impurities and allowed to crystallize by slow evaporation of solvent at room temperature. Good transparent crystals of size around 1.1 cm× 0.5 cm were obtained in a period of about two weeks and are shown in figure1. The crystals were exposed to 100 MeV O^{7+} ions at the 15 UD 16 MV Pelletron Tandem Van de Graff Accelerator at Inter University Accelerator Center (IUAC), New Delhi, India. The experiments were performed at 300 K in the experimental chamber of diameter 1.5 m maintained at 10^{-7} mbar vacuum, with the ion fluencies 1.7×10^{10}, 1×10^{11} and 1.7 $x10^{11}$ ions/cm^2 and its equivalent gamma doses are 1 Mrad, 6 Mrad and 10 Mrad. The typical beam current during irradiation was 0.285 particle nano-ampere (pnA). The range of ions in the crystals is 184 µm. The electronic energy loss is 3740 MeVcm^2/g and nuclear energy loss is 2.03 MeVcm^2/g (25).

3. RESULTS AND DISCUSSION

3.1. Powder X-Ray Diffraction Analysis

The unirradiated and irradiated crystals were subjected to powder X-ray diffraction by using a Rigaku-Miniflex X-ray diffractometer with a scan speed of 5°/min with Cu-Kα radiations (λ=1.5406 Å) in 2θ range from 20° to 80°. The XRD patterns of unirradiated and irradiated LASN crystals are shown in figure 2. The diffraction patterns confirm high degree of crystallinity of the sample. It can be seen from **figure 2** that there is a change in intensity of peaks after irradiation. When grown crystals exposed to ionizing radiation, it will induce significant change in the physical properties of the crystal. The change in relative intensity and the shift in the angular position of peaks can be explained by change in lattice spacing due to ion induced defects in the lattice after irradiation (7, 10). The lattice parameters values of LASN taken from the single crystal XRD analysis (a = 6.127 Å, b = 12.394 Å, C = 5.797 Å (23) were used for the simulation of 'hkl' values and the corresponding ’d’ values have also been calculated. Using the simulated hkl values and the experimental ´d´ values, the lattice parameters were calculated with the help of the computer powder X-ray diffraction program. The crystallite size of unirradiated and irradiated samples was calculated using Scherrer formula

$$L = \frac{K\lambda}{W\cos\theta} \qquad (1)$$

where k = 1, λ = 1.5406 Å and W= full width at half-maxima of the peaks at the diffracting angle. The calculated particle sizes and lattice parameters are given in Table 1. From table 1, it can be seen that, there is no change in the (orthorhombic) phase structure of the irradiated samples; however there are changes in the lattice parameters and crystallite size after irradiation due to compressive strain field generated in the material after irradiation.

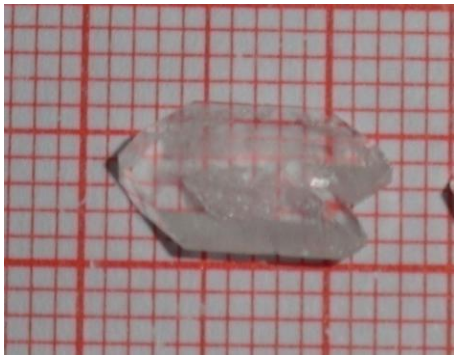

Figure 1. The photograph of the as-grown LASN single crystals.

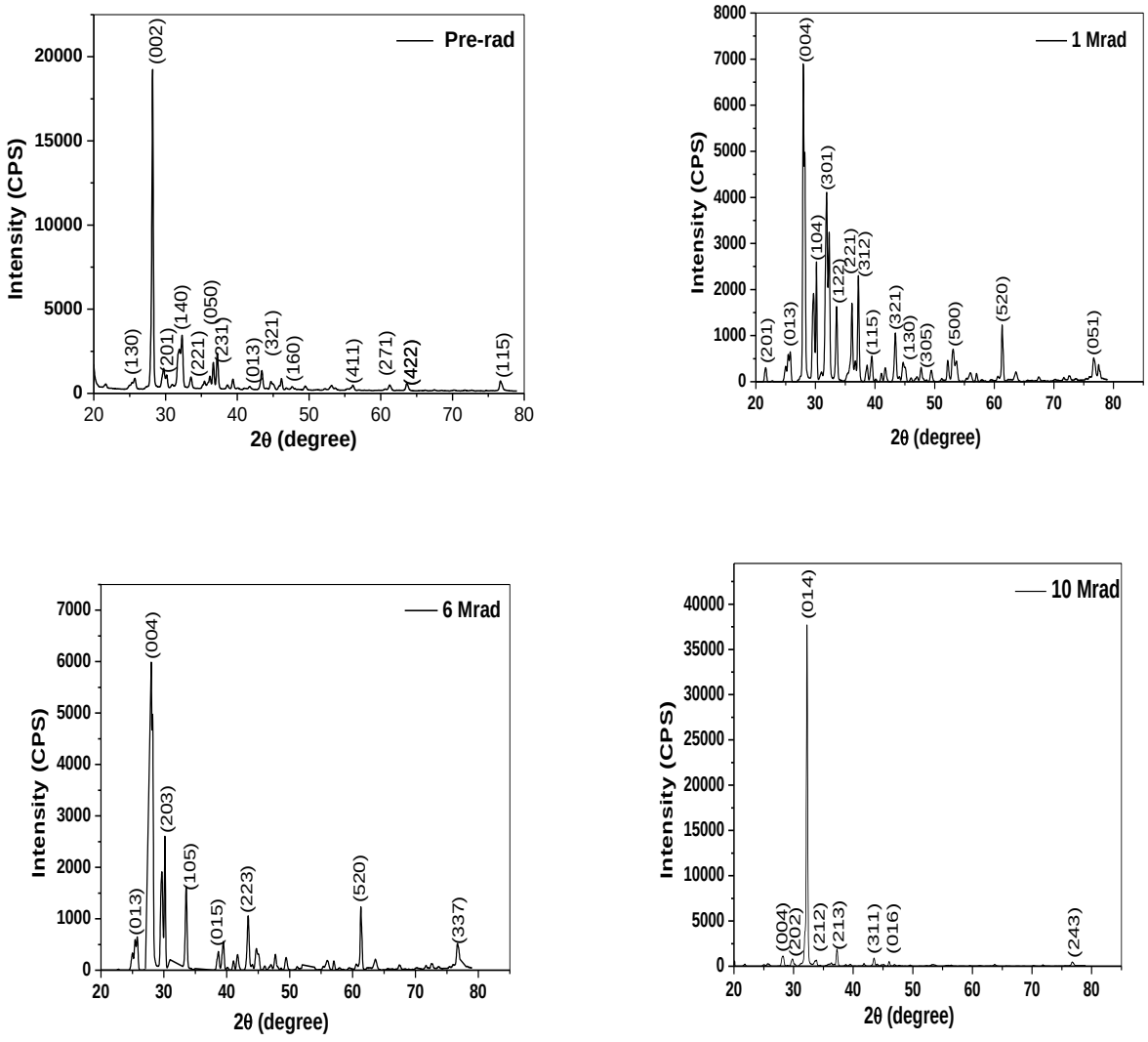

Figure 2. Powder XRD pattern of unirradiated and 100 MeV O^{7+} ion irradiated LASN crystal

Table1 The crystallite size and lattice parameters of unirradiated and irradiated LASN crystals

Dose (Mrad)	crystallite size (nm)	a (Å)	b (Å)	c (Å)	volume ($Å^3$)	crystal structure
Unirradiated	36.3	6.835	12.209	6.352	530.065	Orthorhombic
1	18	8.623	6.235	12.642	683.077	Orthorhombic
6	18.5	8.143	6.675	12.705	690.574	Orthorhombic
10	31.9	6.891	5.621	12.653	490.105	Orthorhombic

3.2. FTIR Spectral Analysis

The infrared spectral analysis provides useful information regarding the molecular structure and functional groups of the compound. The infrared spectrum of unirradiated and irradiated LASN crystals are shown in figure. 3. The spectrum were recorded in the frequency range 400–4000 cm^{-1} using FTIR-8400S spectrophotometer, SHIMADZU model under a resolution of 4 cm^{-1} and with the scanning speed of 2 mm/sec. The asymmetric NH_3^+ stretching vibrations appear at frequency 3088 cm^{-1}. The absorption peak at 1616 cm^{-1} confirms the presence of NH_3 bending. The observed wave numbers and the proposed assignment of the spectrum are shown in table 2. The presence of nitro groups in the spectrum confirms the grown LASN compound (23). It can be seen from figure 3 that, some of the absorption bands are completely destructed after irradiation. The destruction of these bands with irradiation may further enhance the amorphous nature of the sample. The absence of a prominent new peak in irradiated crystals confirms that there is no significant formation of intermediate chemically distinct material during irradiation (10, 26).

3.3 UV–Visible Spectral Analysis

The UV–visible spectrum gives limited information about the structure of the molecule, because the absorption of UV and visible light involves promotion of the electron in the σ and π orbital from the ground state to higher states. Transmittance spectra are very important for any NLO material because a nonlinear optical material can be of practical use only if it has wide transparency window. The unirradiated and irradiated LASN crystals were subjected to UV-Visible studies in the spectral range 200-800 nm, using Perkin-Elmer UV-visible spectrophotometer and the absorption spectra were recorded at the room temperature and are shown in figure 4. It can be observed that there is no absorption of light in the UV–visible range of the electromagnetic spectrum and the UV cutoff wavelength of unirradiated and irradiated LASN is below 300 nm therfore crystals can be used as a potential material for SHG or other applications in the blue and violet regions (23). The optical absorption of LASN crystal wsa found to increase with increase in radiation dose and with increase in dose, a higher concentration of defects may be formed. The increase in absorption may be due to the capture of excited electrons by existing ion vacancies and the formation of additional defect centres. The change in absorption may be also attributed to the creation of some intermediate energy levels due to structural rearrangements. Due to the ion irradiation, there is a change in the absorption edge and almost uniform increase in absorption. Internal structure is not varied after irradiation, as can be evidenced from the absence of any additional peaks in irradiated LASN absorption spectrum (7, 8, 16).

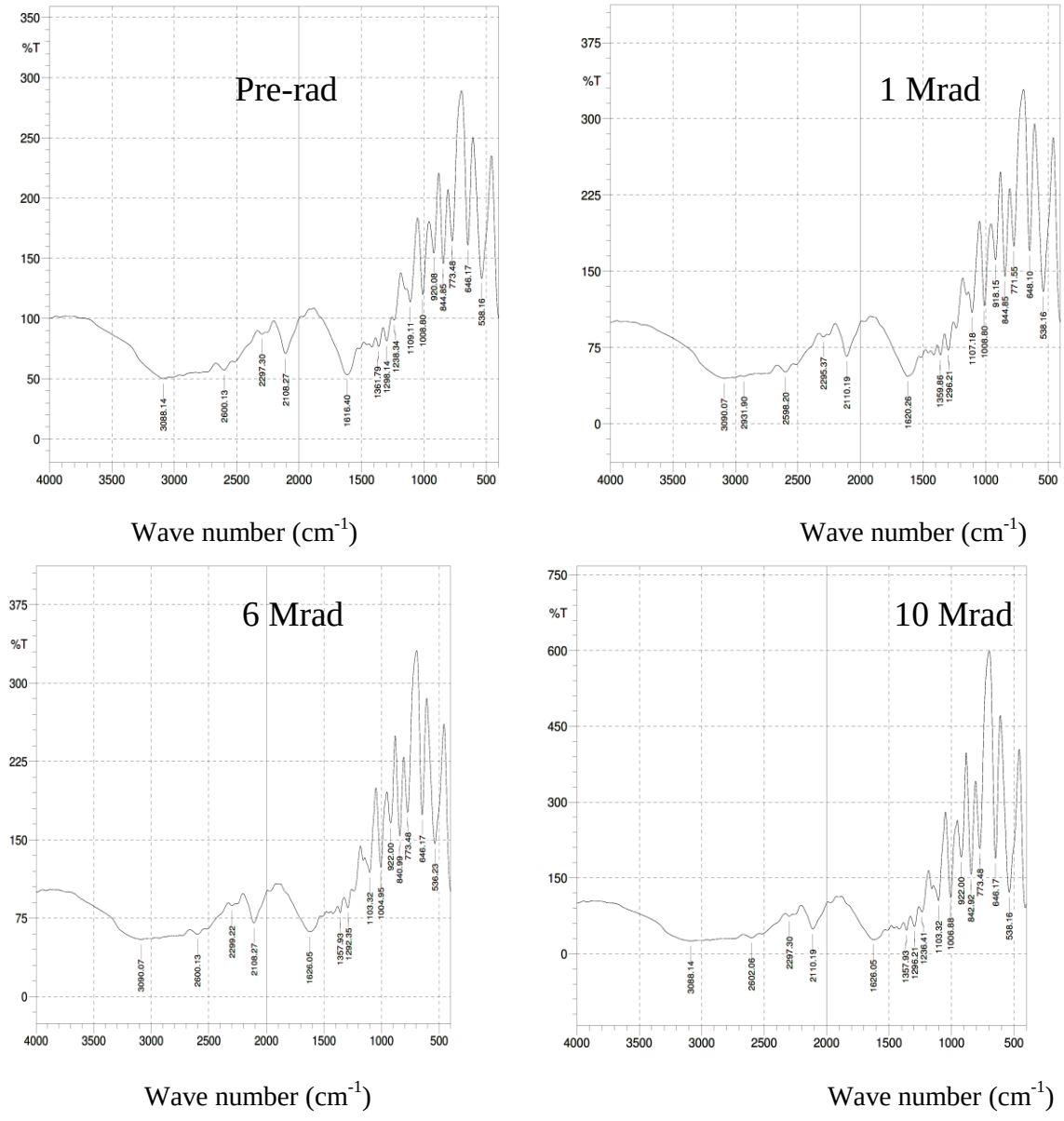

Figure 3. FT-IR spectra of unirradiated and 100 MeV O^{7+} ion irradiated LASN crystals.

Table 2. FT-IR functional group assignments of the grown L-alanine sodium nitrate single crystal.

Wave number (cm^{-1})	Assignment
3088	Asymmetric NH_3^+ stretching
2297	CH_3 stretching
1616	NH_3^+ bending
1362	NO_3 stretching
1238	NH_3^+ rocking
1109	NO_3 stretching
1009	Overtone of torsional oscillation of NH_3^+
920	Overtone of torsional oscillation of NH_3^+
845	NO_3 stretching
774	NO_3 stretching
646	COO^- in plane deformation
538	Torsional oscillation of NH_3^+

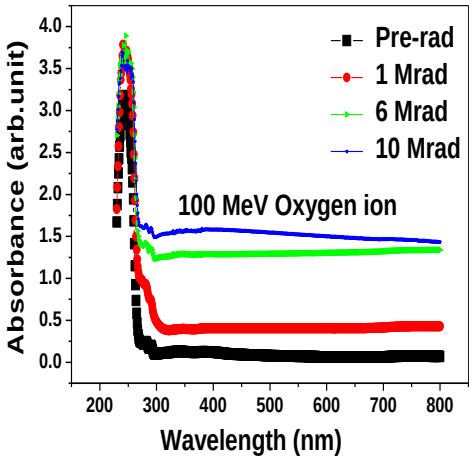

Fig. 4. UV–Vis spectrum of unirradiated and irradiated LASN crystals

3.4. Dielectric Measurement

The dielectric measurement is one of the useful method for characterization of electrical response in crystalline materials. The surfaces of the samples were polished and coated with silver paste while characterize to ensure good electrical contacts. The capacitance and dissipation factor of the unirradiated and irradiated crystals have been measured using High Frequency LCR Meter 6500P in the frequency range from 20 Hz to 10 MHz. The dielectric constant ε_r has been calculated using the equation;

$$\varepsilon_r = \frac{C\,t}{A\,\varepsilon_0} \qquad (2)$$

where $\varepsilon_o = 8.854\times10^{-12}$ F/m is the permittivity of free space, t is the thickness of the sample, C is the capacitance and A is the area of the face of the crystal in contact with the electrode. Figure 5 shows the plot of the dielectric constant versus applied frequency for unirradiated and irradiated LASN crystals. From the figure, it can be seen that the dielectric constant was found to decrease with increase in frequency before and after irradiation. The large values of dielectric constant at low frequency might be attributed to the presence of space charge polarization. The decrease in the values of dielectric constant with the frequency takes place when the jumping frequency of electric charge carriers cannot follow the alternation of the ac electric field applied beyond a certain critical frequency. The dielectric constant was found to increase after irradiation. The increase in dielectric constant may be correlated to the defects created along the ion tracks. These defects cause an increased space-charge contribution which increase the dielectric constant of crystals (7, 8, 14- 18). When the dose is 1 Mrad the damaged regions are isolated from each other when the ion produces a region of amorphous material surrounded by regions containing defects. As the dose increases (6 Mrad and 10 Mrad) there is decrease in the dielectric constant. As the dose increases, high density of extended defects and heavily damaged regions may be formed. These heavily damaged regions overlap and an amorphous layer may be formed. This decreases the density and hence the dielectric constant decreases during subsequent irradiation (27). The dielectric loss may be due to the perturbation of the phonon system by an electric field. The energy transferred to the phonons dissipates in the form of heat (8, 9, 16, 19). The variation of dielectric loss as a function of frequency is shown in figure 6. From the figure, it can be seen that the dielectric loss was found to decrease after irradiation. The ac conductivity σ_{ac} is calculated by substituting the value of dielectric constant ε_r and dielectric loss $\tan\delta$ in the relation:

$$\sigma_{ac} = 2\pi f \varepsilon_o \varepsilon_r \tan\delta \qquad (3)$$

where f is the frequency of the applied field. Figure 7 shows the response of ac conductivity with frequency in the range from 20 Hz to 10 MHz for unirradiated and 100 MeV O^{7+} ions irradiated LASN crystals. From the figure, it can be seen that ac conductivity was found to increase with increase in frequency before and after irradiation. The observed ac conductivity was found to be more at higher frequencies due to a reduction in the space charge polarization. The ac conductivity of the crystal was found to increase after irradiation owing to the fact that more defects are created upon irradiation (10, 18, 28-31).

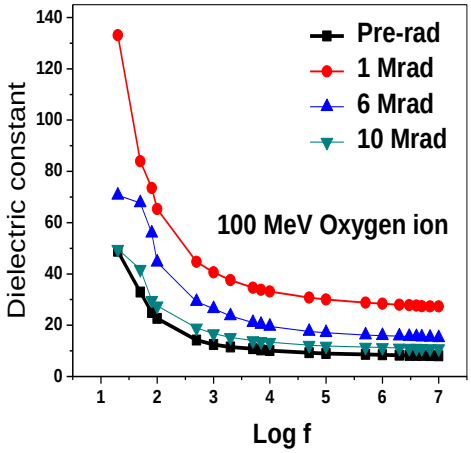

Figure 5. Plot of dielectric constant versus applied frequency for unirradiated and irradiated LASN crystals.

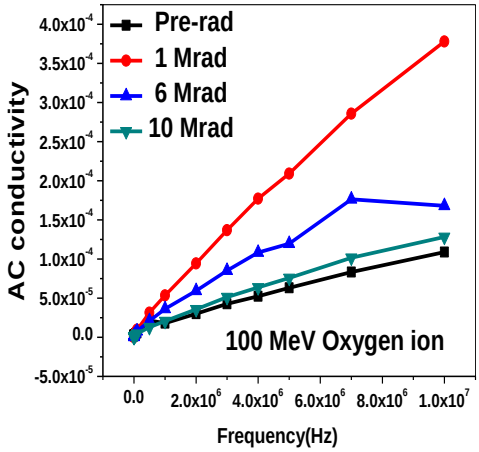

Figure 7 . Variation of ac conductivity versus frequency for unirradiated and irradiated LASN crystals.

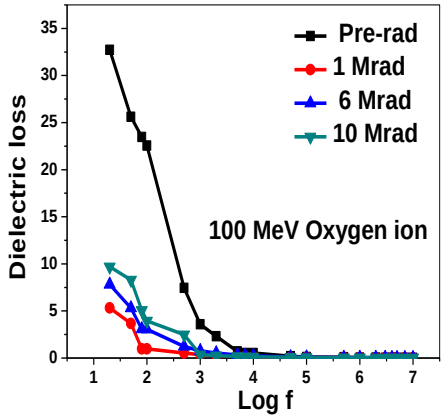

Figure 6. The variation of dielectric loss as a function of frequency for unirradiated and irradiated LASN crystals.

Table 3. DC conductivity values of unirradiated and irradiated LASN crystals.

	Unirradiated	1 Mrad	6 Mrad	10 Mrad
Conductivity $(\Omega.\ m)^{-1}$	1.09×10^{-9}	2.14×10^{-8}	2.43×10^{-8}	2.84973×10^{-8}

3.5. DC Conductivity Study

The dc electrical conductivity study helps to understand the behaviour of charge carriers under a dc field, their mobility and activation energy. The conductivity in ionic crystalline solids is mainly due to the presence of point defects in the lattice and due to different types of mobile charges as given in this relation;

$$\sigma = \sum_i m_i q_i e \mu_i \qquad (4)$$

Where summation is taken over all the charged species (i), (m) indicates the number of mobile charges of the type (i) having net charge ($q_i e$) and (μ_i) represents electrical mobility. The dc conductivity (σ_{dc}) of unirradiated and irradiated crystals was calculated using the relation;

$$\sigma_{dc} = \frac{t}{R A} \qquad (5)$$

where, R is the measured resistance (30, 32-34). The dc conductivity measurement was carried out using Keithley dual channel source meter model 2636A at different temperatures ranging from 300 to 423 K. The I-V characteristic curves of unirradiated and irradiated LASN crystals are shown in Figure 8 and from which the conductance values were calculated. The dc conductivity values are given in table 3 and it can be seen that, the dc conductivity was found to increase with increase in radiation dose due to ion induced defects in crystal lattice (10,18, 28). Figure 9 shows the plot of dc conductivity with temperature for unirradiated and irradiated LASN crystals. From this figure, it can be seen that the dc conductivity was found to increase with increase in temperature before and after irradiation. The conductivity graph exhibits the intrinsic and extrinsic regions. The conductivity at high temperature above 330 K is intrinsic, which is due to the thermally created vacancies and defects created in crystalline lattice. Extrinsic region at low temperatures les than 330 K is a structure-sensitive region i.e., electrical conductivity is controlled by impurities (28, 30, 31, 33- 35). The activation energies for unirradiated and irradiated samples were calculated using the equation;

$$\sigma = \sigma_o \exp\left(\frac{E_a}{K_B T}\right) \qquad (6)$$

$$\ln \sigma = \ln \sigma_o + \left(\frac{E_a}{K_B T}\right) \qquad (7)$$

where E_a is the activation energy, K_B the Boltzmann constant, T is the absolute temperature and σ_o is the constant depending on the material. The value of E_a of unirradiated and irradiated samples were determined from the slope of $\ln \sigma$ versus $\frac{1}{T}$ (figure 10). The activation energies obtained for unirradiated and irradiated LASN crystals are tabulated in table 4.

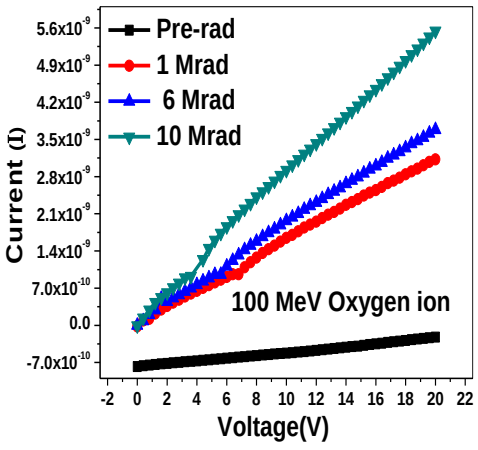

Figure 8. I-V graph of unirradiated and irradiated LASN crystals.

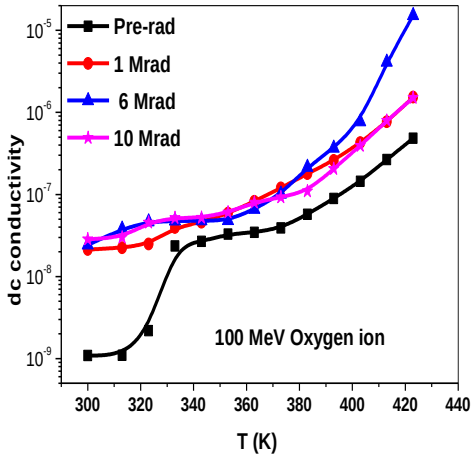

Figure 9. Variation of dc conductivity versus temperature for unirradiated and irradiated LASN crystals.

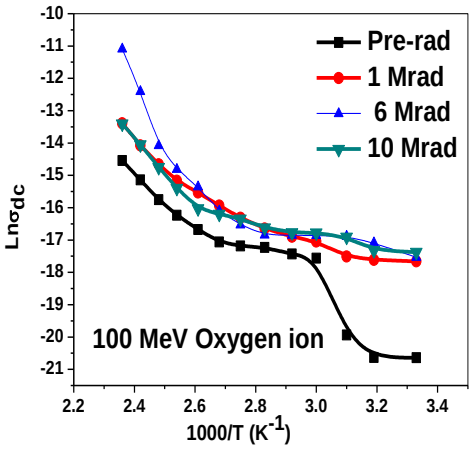

Figure 10. Plot of $\ln \sigma$ versus $\frac{1000}{T}(K^{-1})$ for unirradiated and irradiated LASN crystals.

Table 4. Activation energy of the unirradiated and irradiated LASN crystals.

Dose (Mrad)	Activation energy E_a(eV)
Unirradiated	0.525
1	0.373
6	0.475
10	0.317

3.6. Differential Scanning Calorimetric Studies

The DSC of unirradiated and irradiated LASN crystals were performed using Universal VA.7A TA Instruments DSC Q200 in the temperature range 40 - 320°C at a heating rate of 10°C/min in the nitrogen atmosphere and shown in figure 11. The sharp endothermic peaks at 281.9, 282.7, 283.1 and 288.6°C correspond to the melting point of unirradiated crystal and after 1 Mrad, 6 Mrad and 10 Mrad of total dose respectively. The sharpness of these endothermic peaks shows the good degree of crystallinity of the samples (35). The values of the onset of melt (T_o), melting point (T_m), completing of melt (T_c), heat of fusion (ΔH) and melting range for unirradiated and irradiated LASN crystals are tabulated in table 5. From the table 5 it can be seen that, the melting point remains unaffected after ion irradiation and there is no phase transition before the melting point of the unirradiated and irradiated LASN crystal. Hence, this material has very good thermal stability up to melting point and the does not decompose as a result of irradiation (23). The DSC curves obtained for irradiated crystals are nearly same as that of unirradiated crystal hence, suggesting the same chemical entity in the crystal lattice without any modification in its structure (10, 37).

Table 5 The values of T_o, T_m, T_c, ΔH and melting range for unirradiated and irradiated LASN crystals.

Dose (Mrad)	T_o (°C)	T_m (°C)	T_c (°C)	ΔH (J/g)	Melting range (°C)
Unirradiated	243.6	281.9	303.6	1370	60
1	252.7	282.7	300.7	1250	48
6	248.1	283.1	301.1	1232	18
10	255.4	288.6	302.4	864.4	47

Table 6. Refractive index of the unirradiated and irradiated LASN crystals.

Dose (Mrad)	Polarizing angle(degree)	Refractive index
Unirradiated	56.0	1.48
1	56.0	1.48
6	56.3	1.50
10	56.3	1.51

3.7. Refractive Index (RI) Measurement

Brewster's angle method was used to calculate the RI of unirradiated and irradiated LASN crystals by using a red (He-Ne) laser of 632.8 nm wavelength. The refractive index of unirradiated and 100 MeV O^{7+} ions irradiated LASN crystals was calculated using the equation;

$$RI = \tan\theta_p \qquad (8)$$

where θ_p is the polarizing angle and the results are tabulated in table 6. From the table 6 it can be seen that, the RI was found to increase slightly after irradiation. The increase in RI may be correlated to the defects created after irradiation. These defects offer high refraction for the light travelling through irradiated crystal (14, 11, 15, 37). The modification in the RI due to irradiation implies the possibility of fabricating optical waveguides in these crystals (11, 17, 20-22).

3.8. Microhardness Studies

The microhardness studies were carried out to determine the mechanical strength of the crystal. The polished surface of unirradiated and irradiated LASN crystals were subjected to static indentation tests at room temperature using a Vicker's microhardness tester model HMV-2 Ver 1.02 attached to a large incident light microscope. Loads ranging from 10 to 100 gm were used for making indentations, keeping time of indentation constant at 10 s. The microhardness value was calculated using the equation;

$$H_V = \frac{1.8544\,P}{d^2}\ kg/mm^2 \qquad (9)$$

where, H_V is the Vicker's microhardness number, P is the applied load in kg, d is the average diagonal length of the indentation impression in micrometer and 1.8554 is a constant of a geometrical factor for the diamond pyramid. Figure 12 shows the variation of microhardness values with applied load for both unirradiated and irradiated LASN single crystals. The normal indentation size effect (ISE) involves decrease in hardness value with increasing load and the reverse indentation size effect (RSE) involves increase in hardness values with increasing load. There are many examples of normal occurrence of ISE (7, 38) and RSE (8, 14, 39). From figure 12, it can be seen that the H_V of unirradiated and irradiated LASN crystals increases with load (RSE) and this is due to the elastic nature of the crystal lattice, which will produce the restoring force against the applied load and try to restore the lattice to its original position. Also, H_V increases with increase in radiation dose for all loads, which may be attributed to the increase in density of lattice defects caused by the passage of ions through the LASN lattices. This increased density of lattice defects also produces a residual surface compression stress in the surface layers of the irradiated crystals and thus increasing the hardness of the irradiated single crystals than the unirradiated crystal (14, 40). The Meyer's index number was calculated from Meyer's law, which relates the load and indentation diagonal length,

$$P = kd^n \qquad (10)$$

$$\text{Log } P = \text{Log } k + n \text{ Log } d \qquad (11)$$

where, k is the constant for the given material and 'n' is Meyer's index or work hardening index. To calculate the value of 'n', a graph $\text{Log } P$ versus $\text{Log } d$ is plotted (figure 13) which gives a straight line; the slope of this straight line gives the value

of ' n '. The calculated values of ' n ' are 2.665, 2.614, 2.597 and 2.543 for unirradiated and irradiated LASN crystals after 1 Mrad, 6 Mrad and 10 Mrad respectively. The ' n ' value is in good agreement with the reported value (23). According to Onitsch [41] H_V should increase with P if $n>2$ and decrease if $n<2$ and 'n' should lie between 1 and 1.6 for harder materials and above 1.6 for softer materials. Thus LASN crystal belongs to the soft material category.

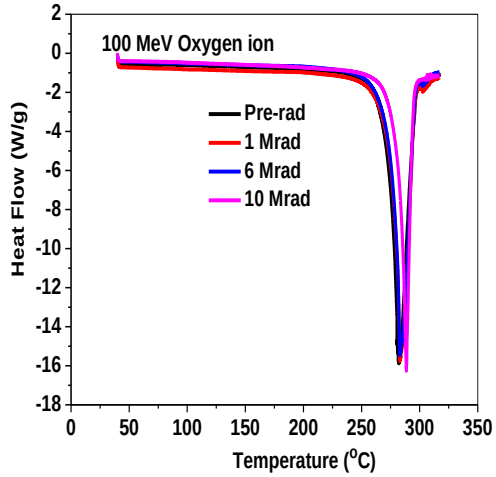

Figure 11. DSC thermograms of unirradiated and irradiated LASN crystals.

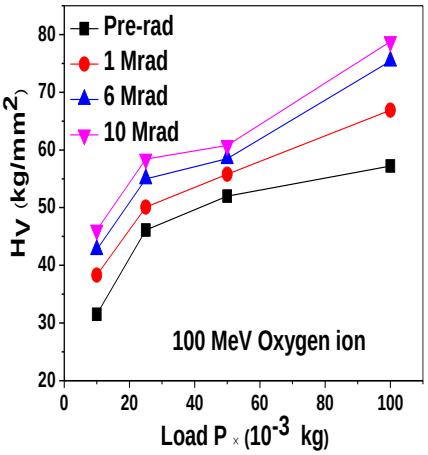

Figure 12. Variation of microhardness values with load for unirradiated and irradiated LASN crystals.

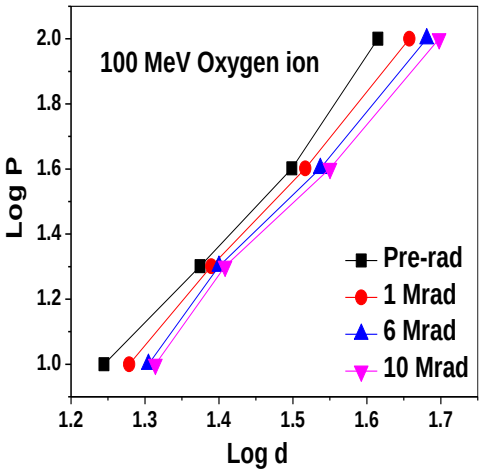

Figure 13. Plot of log P versus log d for unirradiated and irradiated LASN crystals.

Table 7. Comparison of SHG conversion efficiency for unirradiated and irradiated LASN crystals.

Dose (Mrad)	Second harmonic signal (m V)
Unirradiated	5
1	4.7
6	4.2
10	4

3.9. SHG Conversion Efficiency Measurement

The study of nonlinear optical conversion efficiency has been carried out using the modified setup of Kurtz and Perry at the Indian Institute of Science, Bangalore (42). To study the radiation induced effect on nonlinear properties of LASN crystals, the SHG efficiency of irradiated crystal was compared with that of unirradiated crystal. A Q-switched Nd:YAG laser beam of wavelength 1064 nm was used with an input power of 2.15 mJ and pulses width of 10 ns with a repetition rate of 10 Hz. The crystals were powdered and then packed in a micro-capillary of uniform bore and exposed to laser radiations.The second harmonic radiation generated by the randomly oriented microcrystals was focused by a lens and detected by a photomultiplier tube. The optical signal incident on the PMT was converted into voltage output at the cathode ray oscilloscope. The comparison of SHG conversion efficiencies of unirradiated and irradiated crystals are given in table 7. The results show that SHG conversion efficiency of LASN crystals were found to decrease with increase in radiation dose due to lower the laser damage threshold of these crystals (6, 11, 12).

4. CONCLUSIONS

The optical absorption of LASN crystal was found to increase with the increase in radiation dose. The dielectric constant of LASN crystal was found to increase after ion irradiation. AC conductivity strongly depends on frequency and at high frequencies, the conductivity was found to be increase. The present study indicates that the dc conductivity increases with increase in radiation dose and temperature. The DSC curves shows that the melting point remains unaffected after irradiation. The modification in the RI due to irradiation implies the possibility of fabricating optical waveguides in LASN single crystal. The hardness of the crystal enhances for irradiated samples. The SHG decreases with increase in radiation dose.

ACKNOWLEDGEMENTS

The one of the author Mrs. Ahlam Motea is grateful to the UGC for JRF fellowship. The authors are grateful to Dr. Ambuj Tripathi, IUAC, New Delhi and Mr. K.C. Praveen for helping in ion irradiations.

REFERENCES

(1) Chun M. K., Goldberg L. and Weller J. F., Appl. Phys. Lett. 1988, 53(13), 1170-71.
(2) Tao X. T., Yuan D. R., Zhang N., Jiang M. H. and Shao Z. S., Appl. Phys. Lett. 1992, 60 (12), 1415- 17.
(3) Sagawa M., Kagawa H., Kakuta A., Kaji M., Saeki M. and Namba Y., Appl. Phys. Lett. 1995, 66(5), 547 – 49.
(4) Kaczmarek S. M., Zendzian W, Lukasiewicz T, Stepka K., Moroz Z. and Warchol S., Spectrochim. Acta. A. 1998, 54, 2109–16.
(5) Vaddigiri A., Potter K. S., Thomes W. J. and Meister D. C., IEEE Trans. Nucl. Sci. 2006, 53(6), 3882- 88.
(6) Roth U., Tro¨ bs M, Graf T., Balmer J. E. and Weber H. P., Appl. Opt. 2002, 41(3), 464-69.
(7) Kanagasekaran T., Mythili P., Kumar B. and Gopalakrishnan R ., Nucl. Instrum. Meth. B. 2010, 268, 36–41.
(8) Kanagasekaran T., Mythili P., Srinivasan P., Vijayan N., Bhagavannarayana G., Kulriya P. K., Kanjilal D., Gopalakrishnan R. and Ramasamy P. Cryst. Res. Technol. 2007, 42(12) 1376 – 81.
(9) Krishnakumar V., Avasthi D. K., Singh F., Kulriya P. K. and Nagalakshmi R., Nucl. Instrum. Meth. B. 2007, 256, 675–82.
(10) Kanagasekaran T., Mythili P., Srinivasan P., Vijayan N., kanjilal D., Gopalakrishnan R. and Ramasamy P., Mater. Res. Bull. 2008, 43, 852–63.
(11) Aithal P. S., Nagaraja H. S., Rae P. M., Nampoori V. P. N., Vallabhan C. P. G. and Avasthi D. K., Nucl. Instrum. Meth. B. 1997, 129, 217-20.
(12) Aithal P. S., Nagaraja H. S., Rae P. M., Nagarajaa H., Raoa P. M., Avasthib D., Sarmab A., Mater. Chem. Phys. 1997, 54, 991-94.
(13) Dong Y., Xu J., Zhou G., Liangbi S., Xiaodong, Hongjun L.J., Solid. State. Commun. 2007, 141 105–108.
(14) Sangeetha K., Ramesh Babu R., Kumar P., Bhagvannarayana G. and Ramamurthi K. Appl. Surf. Sci. 2011, 257, 7573–78.
(15) Raoa P. M., Nagaraja H. S., Aithal P. S., Avasthi D. K. and Sarma A., Mater. Chem. Phys. 1997, 54, 147-50.
(16) Anandha babu G., Ramasamy P., Vijayan N., Kanjilal D. and Asokan K., Nucl. Instrum. Meth. B. 2008, 266, 5032–36.

(17) Bhat S. I., Rao P. M., Ganesh Bhat, A. P. and Avasthi D. K., Surf. Coat. Tech.2002, 158 – 159, 725–28
(18)Srinivasan P, Kanagasekaran T, Lal D K, Gopalakrishnan R, Ramasamy P., Radiat. Eff. Defect. S. 2008, 163, 693-702.
(19)Srinivasan P., Kanagasekaran T., Kulriya P. K., Lal D. K., Gopalakrishnan R. and Ramasamy P., Nucl. Instrum. Meth. B. 2007, 256, 698–704
(20)Olivares J., García-Navarro A, Méndez A, Agulló-López F, García G, García-Cabañes A, and Carrascosa M, Nucl. Instru. Meth. Phys. Res. B. 2007, 257(1), 765-770.
(21) Chen F, J. Appl. Phys. 2009, 106(8), 081101.
(22) Ren Y, Dong N, Chen F, Benayas A, Jaque D, Qiu F, and Narusawa T, Opt. Lett. 2010 35(19), 3276-3278.
(23) Sethuraman K., Ramesh Babu R., Gopalakrishnan R. and Ramasamy P., Cryst. Growth. Des, 2008, 8(6), 1863-69.
(24) Prabha. D. and Palaniswamy, ijCEPr(international journal of chmical, environmental and pharmaceutical research, 2010, 1(1), 54-60.
(25) Ziegler James F., Ziegler M.D. and Biersack J.P., Nucl. Instrum. Meth. B. 2010, 1818–1823.
(26) Nagabhushana H., Nagabhushana B. M., Lakshminarasappa B. N., Fouran S. and Chakradhar R. P. S. Solid. State. Commun. 2009, 149, 1905-08.
(27) Prabhu S. G., Rao P. M., Avasthi D. K. and Guptha S., Nucl. Instrum. Meth. B. 2001, 174 159-162.
(28) Javidi S., Nia M. E., Aliakbari N., Taheri F., Semiconductor Physics, Quantum Electronics and Optoelectronics, 2008, 11(4), 342-44.
(29) Kar S., Verma S. and Bartwal K. S., Physica B, 2010, 405, 4299–302.
(30) Suresh S., Ramanand A., Mani P., Anand K., Arch. Appl. Sci. Res. 2010, 2(4), 119-127.
(31) Peter A. C., Vimalan M., Sagayaraj P., Kumar T. R. and Madhavan J., Int. J. Chem. Tech. Res, 2010, 2(3), 1445-53
(32) Meena M. and Mahadevan C. K., Arch. Appl. Sci. Res. 2010, 2(6), 185-99.
(33) Assencia A. A. and Mahadevan C. B. Mater. Sci. 2005, 28(5), 415–18.
(34) Priya M., Padma C. M., Freeda T. H., Mahadevan C. and Balasingh C., B. Mater. Sci. 2001, 24(5), 511–14.
(35) Kumari R. A., Chandramani R., B. Mater. Sci. 2003, 26(2), 255–59.
(36) Vasantha K. and Dhanuskodi S., J. Cryst. Growth. 2004, 263, 466–72.
(37) Rao V. and Naseema K., Pramana- J. Phys. 2010, 75(3), 513-22.
(38) Li H., Han Y. H. and Bradt R. C. J. Mater. Sci. 1994, 29, 5641-45.
(39) Gong J., Miao H., Zhao Z. and Guan Z., J. Mater. Sci. Eng. A. 2001, 303, 179-86.
(40) Boudoukha L., Paletto S., Halitim F. and Fantozzi G., Nucl. Instrum. Meth. B. 1997, 122 233–8.
(41) Onitsch, E. M Mikroskopie. 1947, 2, 131-51.
(42) Kurtz S. K. and Perry T. T. j. Appl. Phys. 1968, 39(8), 3798–813.

*****